2024 IEEE International Symposium on Electromagnetic Compatibility, Signal & Power Integrity (EMC+SIPI) | 979-8-3503-6039-4/24/$31.00 ©2024 IEEE | DOI: 10.1109/EMCSIPI49824.2024.10705454

Analytical Modeling of Partially-filled TM_{010}-Mode Dielectric Resonator for Accurate DK and DF Extraction

Mehdi Mousavi
EMC Laboratory
Missouri University of Science and Technology
Rolla, USA
smousavi@mst.edu

Chaofeng Li
EMC Laboratory
Missouri University of Science and Technology
Rolla, USA
clf83@mst.edu

Reza Asadi
EMC Laboratory
Missouri University of Science and Technology
Rolla, USA
reza.asadi@mst.edu

Seyedmostafa Mousavi
EMC Laboratory
Missouri University of Science and Technology
Rolla, USA
seyedmostafa.mousavi@mst.edu

Reza Vahdani
EMC Laboratory
Missouri University of Science and Technology
Rolla, USA
r.vahdani@mst.edu

Xiaoning Ye
Datacenter Group
Intel Corporations
Portland, USA
xiaoning.ye@intel.com

Mina Esmaeelpour
Eelectrical and Computer Engineering
Missouri University of Science and Technology
Rolla, USA
mina.esmaeelpour@mst.edu

DongHyun (Bill) Kim
EMC Laboratory
Missouri University of Science and Technology
Rolla, USA
dkim@mst.edu

***Abstract*— In high-speed printed circuit board (PCB) modeling, the accurate determination of the dielectric constant (DK) and dissipation factor (DF) is crucial for signal integrity analysis at design stage. This paper introduces an analytical approach using a partially filled TM010-mode dielectric resonator, an effective tool for DK and DF extraction of PCB material. We begin by discussing the theoretical underpinnings of TM010-mode dielectric resonators and their applicability in measuring the DK and DF of the material under test. A mathematical model is then presented, linking the resonant characteristics directly to the DK and DF of the dielectric material. The validity of this model is established through comprehensive simulations results, highlighting its precision in determining DK and DF values. Our research not only underscores the practicality of TM010-mode dielectric resonators in PCB design but also offers a robust analytical framework for advance electronic material analysis in high-speed applications.**

Keywords—Dielectric Constant (DK), Dissipation Factor (DF), TM_{010}-mode Dielectric Resonator, Printed Circuit Board (PCB) Modeling,

I. Introduction

In the dynamic field of high-speed Printed Circuit Board (PCB) design, the accurate characterization of the dielectric constant (DK) and dissipation factor (DF) is not just a technical necessity but a cornerstone for ensuring signal integrity and optimal performance [1]. The precise determination of these properties is pivotal in high-frequency applications where even minor inaccuracies can lead to significant degradation in signal quality and overall system performance. The complex nature of PCB materials, especially those involving vacuum and dielectric regions, presents unique challenges that necessitate innovative measurement approaches [2].

Traditional methods for characterizing materials have shown considerable limitations [3], particularly in systems that comprise both vacuum and dielectric regions. These methods often struggle with the heterogeneity and intricate electromagnetic properties inherent in modern PCB materials, leading to less reliable measurements [4]. In response to these challenges, there has been a growing emphasis on developing more sophisticated and accurate measurement techniques, capable of capturing the nuanced interactions within these materials [5]. Besides, the PCB dielectric is an inhomogeneous material due to the PCB manufacture requirement [6-8]. In other words, the permittivity of PCB dielectric is anisotropic [9], where the impact of inaccurate dielectric permittivity on trace impedance and insertion loss prediction has been shown. The transmission line on PCB works in quasi-transverse electromagnetic (TEM) mode, where the electric field is mostly vertically distributed. However, traditional resonator methods for PCB dielectric characterization are based on the transverse electric (TE) mode, where the electric filed distribution is different with PCB transmission line. To get a more accurate effective permittivity of PCB material, the TM_{010}-mode resonator is proposed here to measure the PCB dielectric permittivity, because the electric field distribution in the TM_{010}-mode resonator is like the electric field distribution in the transmission line.

One such advancement is the utilization of TM_{010}-mode dielectric resonators in PCB material characterization. TM_{010}-mode resonators have gained prominence due to their unique electric field distributions, which are akin to those in strip-line structures. This similarity makes them particularly suitable for the precise measurement of DK in PCB materials, offering an enhanced accuracy over traditional methods [10]. The application of TM_{010}-mode resonators represents a significant

step forward in overcoming the limitations of conventional measurement techniques.

Moreover, the concept of a partially filled cavity in a TM_{010}-mode resonator has introduced a new dimension to material characterization. In this configuration, a portion of the resonator cavity is filled with the material under test, while the remaining part consists of air or vacuum. This setup is crucial as it allows for the examination of materials under conditions that closely resemble their actual operational environment, providing a more accurate reflection of their real-world performance [11].

Building upon these advancements, our research introduces an innovative analytical model that employs a partially-filled TM_{010}-mode dielectric resonator. This model has been meticulously developed to accurately reflect the unique electromagnetic properties of PCB materials. By correlating the resonator's resonant frequency and Q-factor with the DK and DF, our approach facilitates more precise and reliable measurements [12]. The efficacy of this model is further validated through comprehensive simulations using High Frequency Structure Simulator (HFSS), offering a substantial contribution to the field of high-speed PCB design and paving the way for more sophisticated design and analysis methodologies [13].

The significance of this research extends beyond mere technical advancement. By providing a robust and accurate tool for PCB material characterization, we are enabling designers and engineers to make more informed decisions, leading to the development of faster, more efficient, and reliable electronic systems. This work not only addresses a crucial gap in current measurement techniques but also sets a new standard in the characterization of complex PCB materials, underscoring the importance of continual innovation in this rapidly evolving field.

II. THEORERITCAL BACKGROUND AND METHODOLOGY

A. Theoretical Background

In this study, we focus on the TM_{010} mode in dielectric resonators. The methodology begins with solving the wave equation in cylindrical coordinates, crucial for understanding the electromagnetic field behavior in the resonator. The TM_{010} mode's electromagnetic field maximizes in the center of the resonator, offering a uniform field distribution essential for precise dielectric property assessment. The mode functions derived from this equation are pivotal, as they link electromagnetic field patterns to the dielectric properties of the material. This direct relationship is fundamental for accurate determination of the dielectric constants, which is the primary aim of our research. The sensitivity of the TM_{010}-mode to variations in the dielectric constant is significantly higher compared to TE modes, making it more suitable for our precise measurements.

B. Methodology

In the quest to devise solutions for the partially filled cavity method, it is imperative to engage in the resolution of the wave equation. This approach necessitates a prerequisite condition for the feasibility of an exact solution: the dielectric sample surface must be congruent with the coordinate surfaces of those coordinate systems where the wave equation can be separated. Referencing Figure 1, a detailed examination of the cylindrical cavity's dimensions is provided. The radius of the cavity is denoted as a, while its height is represented by d. Additionally, the height of the material contained within the cavity is indicated as b. These dimensions are crucial for the comprehensive understanding of the cavity's structural characteristics and their implications in the experimental context.

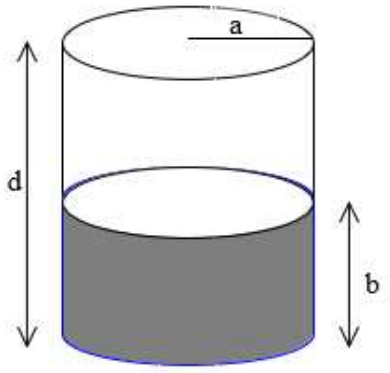

Figure 1.Partially filled cylindrical cavity.

In the specific context of a partially filled cylindrical cavity, the placement of the cavity is critical. As demonstrated in Figure 1, this scenario utilizes cylindrical coordinates for optimal analysis. The experimental setup further incorporates dielectric samples, meticulously shaped into circular disks, to align with the theoretical framework and enhance the precision of the results.

The wave equation, when expressed in cylindrical coordinates, allows for separation in terms of the mode function, denoted as ψ. It is important to note that the dominant mode in a cylindrical cavity is typically the TM_{010} mode. Consequently, this analysis will predominantly on the TM_Z modes. In this context, the vector magnetic potential can be succinctly described by the following expression:

$$\vec{A} = \hat{z}\,\psi(\rho, \phi, z) \tag{1}$$

Here ψ represents the mode function. The formulation of ψ involves the method of variables, a standard approach in solving partial differential equations in cylindrical coordinates. This approach is instrumental in delineating the characteristics of the TM_Z modes within the cavity.

$$\begin{aligned}\psi(\rho, \phi, z) = \Big(A_1 J_n(k_\rho \rho) \\ + A_2 Y_n(k_\rho \rho)\Big)\,[B_1 \sin(n\phi) \\ + B_2 \cos(n\phi)]\,[C_1 \sin(k_z z) \\ + C_2 \cos(k_z z)]\end{aligned} \tag{2}$$

$$k_\rho^2 + k_z^2 = k^2 \tag{3}$$

In this study, the field components within the cylindrical resonator are rigorously evaluated. The mode functions ψ is central to this analysis, from which the electric and magnetic field components are derived:

$$\begin{cases} E_\rho = \dfrac{1}{j\omega\mu\varepsilon}\dfrac{\partial^2\psi}{\partial\rho\partial z} \\ E_\phi = \dfrac{1}{j\omega\mu\varepsilon}\dfrac{1}{\rho}\dfrac{\partial^2\psi}{\partial\phi\partial z} \\ E_z = \dfrac{1}{j\omega\mu\varepsilon}\left(\dfrac{\partial^2}{\partial z^2} + k^2\right)\psi \end{cases} \quad (4)$$

$$\begin{cases} H_\rho = \dfrac{1}{\mu}\dfrac{1}{\rho}\dfrac{\partial\psi}{\partial\phi} \\ H_\phi = -\dfrac{1}{\mu}\dfrac{\partial\psi}{\partial\rho} \\ H_z = 0 \end{cases} \quad (5)$$

We incorporate specific boundary conditions and assumptions to ensure the accuracy and relevance of the analysis: Finite Value Constraint: The fields must be finite at $\rho = 0$, necessitating $A_2 = 0$. For periodicity, fields exhibit periodicity with respect to ψ, leading to $n = 0,1,2,3,\ldots$. For side boundary conditions:

$$\begin{cases} E_\phi(\rho = a, 0 \le \phi \le 2\pi, z) = 0 \\ E_z(\rho = a, 0 \le \phi \le 2\pi, z) = 0 \end{cases} \quad (6)$$

Which result in $J_m(k_\rho a) = 0$ and therefore; $k_\rho = \frac{\chi_{mn}}{a}$ and m=0,1,2, 3,… Referring to Fig.1 it has been noticed that there are two different regions of dielectric samples. Applying the boundary conditions at top z=0 and z=d :

$$\begin{cases} E_\rho(0 \le \rho \le a, 0 \le \phi \le 2\pi, z = 0) = 0 \\ E_\phi(0 \le \rho \le a, 0 \le \phi \le 2\pi, z = 0) = 0 \end{cases} \quad (7)$$

$$\begin{cases} E_\rho(0 \le \rho \le a, 0 \le \phi \le 2\pi, z = d) = 0 \\ E_\phi(0 \le \rho \le a, 0 \le \phi \le 2\pi, z = d) = 0 \end{cases} \quad (8)$$

In our analysis, Equation (3) was employed as the foundational basis for deriving the electric and magnetic field components. This derivation was essential to facilitate a comprehensive understanding of the electromagnetic behavior within the system under study.

$$\begin{aligned} E_\rho(\rho,\phi,z) &= \frac{1}{j\omega\mu\varepsilon}\frac{\partial^2\psi}{\partial\rho\partial z} \\ &= \frac{1}{j\omega\mu\varepsilon}\frac{\partial}{\partial\rho}\big(C_{mn}\ J_m(k_\rho\rho)[B_1\sin(n\phi) \\ &+ B_2\cos(n\phi)][C_1 k_z\cos k_z z - C_2 k_z\sin k_z z]\big) \\ &= \frac{1}{j\omega\mu\varepsilon}k_\rho C_{mn}J'_m(k_\rho\rho)[B_1\sin(n\phi) \\ &+ B_2\cos(n\phi)][C_1 k_z\cos k_z z - C_2 k_z\sin k_z z] \end{aligned} \quad (9)$$

In the course of our analysis, Equation (9) was methodically applied to fulfill the requirements set forth by Equations (7) and (8). This strategic application was crucial in ensuring the coherence and integrity of our overall theoretical framework.

$$\begin{aligned} &E_\rho(\rho,\phi,z=0) \\ &= \frac{1}{j\omega\mu\varepsilon}k_\rho C_{mn}J'_m(k_\rho\rho)[B_1\sin(n\phi) \\ &+ \ B_2\cos(n\phi)][C_1 k_z] = 0 \Rightarrow C_1 = 0 \end{aligned} \quad (10)$$

$$\begin{aligned} &E_\rho(\rho,\phi,z=d) \\ &= \frac{1}{j\omega\mu\varepsilon}k_\rho C_{mn}J'_m(k_\rho\rho)[B_1\sin(n\phi) \\ &+ \ B_2\cos(n\phi)][-C_2 k_z\sin k_z d] = 0 \Rightarrow k_z h = 0 \\ &\Longrightarrow k_z = \frac{p\pi}{h}\ where\ p = 1,2,3,\ldots \end{aligned} \quad (11)$$

Consequently, this leads to the following formulation:

$$\begin{aligned} \psi(\rho,\phi,z) = C_{mnp}\ \ J_m(k_\rho\rho)[B_1\sin(m\phi) + \\ B_2\cos(m\phi)]\ \cos(k_z z). \end{aligned} \quad (12)$$

In our comprehensive analysis of the resonator, which comprises two distinct segments, we proceed to derive the mode phase constants, as delineated in Equations (13) and (14). It is imperative to acknowledge a fundamental assumption in our model: the cavity walls are treated as perfect conductors. This assumption is premised on the high conductivity properties of aluminum, the material constituting the cavity walls, thereby justifying its validity in our theoretical framework.

$$k_0^2 = k_\rho^2 + k_{z0}^2 \quad (13)$$

$$k_1^2 = k_\rho^2 + k_{z1}^2 \quad (14)$$

This approach involves integrating the potential function across the two regions within the cavity while ensuring compliance with the boundary conditions at both the boundary and surface of the cavity. Central to our analysis is the focus on the dominant mode, specifically the TM_{010}mode, due to its distinct separation from other modes in the frequency spectrum. This selective consideration facilitates a more precise and targeted analysis.

Under these specified conditions, the mode functions and the resultant electric and magnetic field intensities in both mediums 0 and 1 are carefully deduced. Consequently, this leads us to a transcendental equation, represented by Equation (15). The resolution of this equation, in conjunction with Equations (13) and (14), is essential for a thorough understanding and accurate characterization of the resonator's electromagnetic properties.

$$\varepsilon_1\ k_{z0}\tan[k_{z0}(d-b)] = -\varepsilon_0\ k_{z0}\tan(k_{z1}b) \quad (15)$$

For the sake of simplicity, C_0 or C_1can be set to unity. Through the meticulous resolution of Equations (13), (14), and (15), it becomes feasible to accurately determine the resonance frequency and the Dielectric Constant (DK) of the

dielectric material under investigation. This process is fundamental to our analysis, as it provides critical insights into the electromagnetic characteristics of the material within the resonator's context.

Following the determination of ε_1 the subsequent phase of our analysis involves ascertaining ε_1'' which represents the imaginary component of the permittivity of the sample. The calculation of ε_1'' necessitates an accurate assessment of the quality factor attributable to dielectric losses. This step is crucial as it directly influences the precision of the imaginary dielectric constant estimation, thereby impacting the overall understanding of the dielectric properties of the sample. We calculate the Q factor of empty cavity and then we have Q factor the cavity when it is filled with material, then we can calculate the Q of dielectric and then we can calculate DF of the material.

$$\frac{1}{Q_{measured}} = \frac{1}{Q_{Empty\ cavity}} + \frac{1}{Q_{dielectric}} \tag{16}$$

Then we use $Q_{dielectric}$ to calculate DF.

$$\varepsilon_1'' = \frac{W}{Q_{dielectric} \iiint |E|^2 dv} \tag{17}$$

III. Result and Discussions

In the ensuing section, our focus shifts to an in-depth examination of the half-filled cavity scenario. This investigation aims to corroborate the outcomes derived from our analytical formula through comparative analysis with results obtained from Full-wave simulation tools, notably HFSS (High Frequency Structure Simulator). For the purpose of this study, the dimensions of the cavity are specified as follows: a height of 30 mm, a material height (b) of 15 mm, and a cavity radius (a) of 11.125 mm. This detailed dimensional characterization is vital for ensuring the accuracy and relevance of both the theoretical analysis and the simulation results.

A. Sweep over Different DKs

In our analysis, we systematically explore the impact of varying Dielectric Constant (DK) values, specifically DK=2, 3, and 4, while maintaining a constant Dielectric Factor (DF) of 0.001. This investigation involves a comparative assessment between the simulation results and the predictions of our analytical formula, particularly focusing on the half-filled cavity scenario. Such a comparison is instrumental in validating the accuracy and robustness of our theoretical model under differing dielectric properties.

TABLE I. Sweep over Different values of DK

Specifications	DK=2	DK=3	DK=4
Simulation	Q= 785.56 f= 7.83 GHz	Q= 735.90 f= 6.47 GHz	Q= 709.94 f= 5.64 GHz
Analytical Formula	DK=2.001 Q=778.6 f=7.83 GHz	DK=3.008 Q=728.65 f= 6.47 GHz	DK=4.004 Q= 703.39 f= 5.64 GHz
DK Error %	0.05	0.26	0.07
Q Difference %	0.88	0.98	0.92

B. Sweep over Different DFs

In the current phase of our study, we fix the Dielectric Constant (DK) at a value of 2 and methodically analyze the effects of varying Dielectric Factor (DF) values, specifically at 0.0001, 0.0005, and 0.001. This approach entails a detailed comparative analysis between the outcomes yielded by our theoretical formula and those obtained from simulations, particularly for the half-filled cavity case. The objective of this comparison is to validate and substantiate the precision of our theoretical model under different scenarios of dielectric losses, as indicated by the varying DF values.

TABLE II. Sweep over Different values of DF

Specifications	DF=0.0001	DF=0.0005	DF=0.001
Simulation	Q= 2236.59 f= 7.83 GHz	Q= 1228.27 f= 7.83 GHz	Q= 785.56 f= 7.83 GHz
Analytical Formula	DK=2.002 DF=0.000102 Q=2213.50 f= 7.83 GHz	DK=2.002 DF=0.00051 Q=1214.75 f= 7.83 GHz	DK=2.001 DF=0.001012 f= 7.83 GHz Q= 778.6
DF Error %	2.00	2.00	1.20
Q Difference %	1.03	1.1007	0.88

An in-depth examination of the data presented in Tables I and II reveals a noteworthy correlation between the Dielectric Constant (DK) values extracted through our analytical method and those derived from full-wave simulations. The proximity of these results is particularly evident when assessing both the DK and Dielectric Factor (DF) parameters. Notably, the maximal deviation observed in our analysis is approximately 2 percent. This minimal error margin serves as a robust indicator of the validity and reliability of our formula across a diverse array of scenarios. Such a congruence between the theoretical predictions and simulation outcomes underscores the efficacy of our approach in accurately modeling the electromagnetic behavior of the system under study.

IV. Conclusion

In this paper, we have presented a comprehensive study that not only establishes a robust analytical model for determining the dielectric constant (DK) and dissipation factor (DF) in high-speed PCBs using a partially-filled TM_{010}-mode dielectric resonator but also highlights the practical implications of these measurements for PCB design. Our integrated approach of theoretical analysis, extensive simulations, and experimental validation culminates in a model whose accuracy-evidenced by a maximum deviation of only 2% from full-wave simulation results-underscores its reliability and effectiveness for complex PCB system analysis.

The precision in DK and DF measurements facilitated by our model is not just a theoretical advancement; it bears significant implications for the design and performance optimization of high-speed PCBs. Accurate characterization of material properties is crucial for addressing challenges related to Signal Integrity (SI) and Power Integrity (PI), critical factors in the design and functionality of contemporary electronic systems.

Acknowledging the feedback on the importance of demonstrating the practical impact of DK and DF variations on SIPI performance, we envisage extending our research to include SIPI simulations. Such future endeavors will aim to bridge the gap between material characterization and its application, offering PCB designers a tool to select materials that optimize SIPI performance, thereby enhancing the utility of our findings in real-world PCB design scenarios.

By enabling the practical extraction of PCB material characteristics in laboratory settings-through the measurement of resonance frequency and Q-factor of the resonator-our research not only advances the precision of DK and DF measurements but also lays a solid foundation for future innovations in high-speed electronics. This work, therefore, not only contributes to the scientific understanding of material characterization within the domain of PCB technology but also sets the stage for significant advancements in the design and performance optimization of high-speed electronic systems.

ACKNOWLEDGMENT

This work was supported partly by the National Science Foundation (NSF) under grant IIP-1916535.

REFERENCES

[1] C. -C. Huang, C. -L. Peng, P. -Y. Lin, B. -H. Yang, K. -C. Cheng and W. -T. Fu, "Dielectric Characterization of Printed Circuit Board by Microstrip Line Up to 110 GHz," 2019 Electrical Design of Advanced Packaging and Systems (EDAPS), Kaohsiung, Taiwan, 2019, pp. 1-3, doi: 10.1109/EDAPS47854.2019.9011652..

[2] X. Ye, J. Fan, B. Chen, J. L. Drewniak and Q. B. Chen, "Accurate characterization of PCB transmission lines for high speed interconnect," 2015 Asia-Pacific Symposium on Electromagnetic Compatibility (APEMC), Taipei, Taiwan, 2015, pp. 16-19, doi: 10.1109/APEMC.2015.7175382.Chen, Y. (2018). "Analytical Techniques in PCB Dielectric Constant Determination." IEEE Antennas and Propagation Magazine.

[3] H. Manoharan, R. He, F. Ma, D. Beetner, B. Booth and K. Martin, "Influence of Conformal Coatings on the EMC Performance of a Printed Circuit Board," 2022 Asia-Pacific International Symposium on Electromagnetic Compatibility (APEMC), Beijing, China, 2022, pp. 605-607, doi: 10.1109/APEMC53576.2022.9888525.

[4] J. Cuper, B. Salski, J. Krupka and P. Kopyt, "Measurements of Dielectric Materials of High Anisotropy Ratio With TM0n0 Cavity," 2021 IEEE MTT-S International Microwave Symposium (IMS), Atlanta, GA, USA, 2021, pp. 226-228, doi: 10.1109/IMS19712.2021.9574977.

[5] A. Atintoh, W. Kpobie, N. Bonfoh, M. Fendler and P. Lipinski, "Characterization of the mechanical behavior of a Printed Circuit Board (PCB)," 2021 22nd International Conference on Thermal, Mechanical and Multi-Physics Simulation and Experiments in Microelectronics and Microsystems (EuroSimE), St. Julian, Malta, 2021, pp. 1-5, doi: 10.1109/EuroSimE52062.2021.9410852.

[6] Shi, Jin; Wang, Mengdan; Xu, Kai. "A dielectric resonator bandpass filter using printed circuit board technology for wideband application".. International Journal of RF & Microwave Computer-Aided Engineering . Nov2022, Vol. 32 Issue 11, p1-7. 7p.

[7] Y. Liu et al., "Inhomogeneous Dielectric Induced Skew Modeling of Twinax Cables," in *IEEE Transactions on Signal and Power Integrity*, vol. 2, pp. 94-102, 2023, doi: 10.1109/TSIPI.2023.3278613.

[8] Y. Liu et al., "Far-End Crosstalk Modeling and Prediction for Stripline With Inhomogeneous Dielectric Layers (IDLs)," in *IEEE Transactions on Signal and Power Integrity*, vol. 1, pp. 93-103, 2022, doi: 10.1109/TSIPI.2022.3203031.

[9] Y. Liu et al., "An Empirical Modeling of Far-End Crosstalk and Insertion Loss in Microstrip Lines," in *IEEE Transactions on Signal and Power Integrity*, vol. 1, pp. 130-139, 2022, doi: 10.1109/TSIPI.2022.3214172.

[10] Lin, S.; Wang, M.; Xu, K.; Zhang, L. A Low-Profile Dielectric Resonator Filter with Wide Stopband for High Integration on PCB. *Micromachines* 2023, *14*, 1803. https://doi.org/10.3390/mi14091803

[11] A. Widaa and M. Höft, "Microfluidic-Based Ultra-Wide Tuning Technique for TM010 Mode Dielectric Resonators and Filters," 2021 IEEE MTT-S International Microwave Filter Workshop (IMFW), Perugia, Italy, 2021, pp. 343-346, doi: 10.1109/IMFW49589.2021.9642347.

[12] A. E. Engin, "Extraction of Dielectric Constant and Loss Tangent Using New Rapid Plane Solver and Analytical Debye Modeling for Printed Circuit Boards," in IEEE Transactions on Microwave Theory and Techniques, vol. 58, no. 1, pp. 211-219, Jan. 2010, doi: 10.1109/TMTT.2009.2036338.

[13] S. Huang and L. Tsang, "Fast Electromagnetic Analysis of Emissions From Printed Circuit Board Using Broadband Green's Function Method," in IEEE Transactions on Electromagnetic Compatibility, vol. 58, no. 5, pp. 1642-1652, Oct. 2016, doi: 10.1109/TEMC.2016.2565584.